

Optical response of YbS and YbO at high pressures and the pressure-volume relation of YbS

K. Syassen, H. Winzen, H. G. Zimmer, and H. Tups

Physikalisches Institut III, Universität Düsseldorf, D-4000 Düsseldorf 1, Federal Republic of Germany

J. M. Leger

Laboratoires de Bellevue, Centre National de la Recherche Scientifique, F-92190 Meudon, France

(Received 1 April 1985)

Reflection spectra of YbS have been measured from 0.5 to 3.5 eV at pressures up to 400 kbar. The optical response indicates the onset of a $4f$ -shell instability near 100 kbar, which is further supported by lattice-parameter measurements. The optical reflectivity differs considerably from that of intermediate-valence (IV) compounds of Sm and Tm. A pronounced absorption band in the near-infrared spectral range, which is also observed in YbO, provides evidence for a localized d component in the IV ground state of both YbS and YbO.

I. INTRODUCTION

In the divalent rare-earth monochalcogenides (RX , $X=O, S, Se, Te$) the localized $4f$ state falls in the gap between valence and conduction band. On applying pressure, the enthalpy difference between divalent and trivalent ground state (with ionic configurations $4f^{n+1}$ and $4f^n5d$, respectively) decreases and simultaneously the optical excitation energy from the $4f^{n+1}$ state to empty d -like states near the conduction-band edge becomes smaller.^{1,2} The pressure-induced $4f$ - $5d$ energetic overlap results in the formation of an intermediate-valence (IV) ground state,^{1,3,4} where the $4f$ shell of each rare-earth (RE) ion has a noninteger occupation. The SmX and TmX have been investigated extensively (see, e.g., Refs. 3–8), because IV behavior is induced at moderate pressures or by chemical alloying. Among the striking properties associated with the $4f$ instability in SmX and TmX , one finds a lattice collapse or bulk modulus softening¹ and a high metallic-like reflectivity below a photon energy of roughly 2 eV.^{9–15}

The EuX and YbX are more stable in their divalent configuration, because the third ionization potential of Eu and Yb is roughly 1.5 eV larger compared with Sm and Tm.¹⁶ This difference results in a larger energetic separation between $4f$ and $5d$ states in the compound, and much higher pressures are involved in inducing a $4f$ - $5d$ energetic overlap in some of the EuX and YbX .^{15,17–21} Among the IV materials the YbX are almost unique through the combination of two properties: (i) The two $4f$ configurations of Yb which are involved in the configuration mixing have a very simple $4f$ multiplet structure.²² (ii) In contrast to IV Yb-intermetallics, two Yb valence electrons are transferred into anion-derived p states, which are separated by several eV from the conduction band.

In this work we are mainly concerned with the optical detection and characterization of the pressure-induced $4f$ instability in YbS at 300 K, but also report on lattice parameter measurements of YbS and on the optical reflectivity of YbO under pressure. The $4f$ -to- $5d$ excitation threshold in YbS at normal pressure is about 1.2 eV.^{23,24}

The optical properties indicate a $4f$ - $5d$ energetic overlap near 100 kbar. A compression anomaly supports the onset of a noticeable change in ionic valence starting near 100 kbar. Above 150 kbar the optical response of YbS shows a pronounced absorption band in the near-infrared (NIR) spectral range (0.5 eV $< \hbar\omega < 1$ eV), which is in marked contrast to the high metallic-like reflectivity of IV SmX and TmX . A similar observation is made in YbO. The way, in which this absorption band evolves with pressure, provides evidence for localized d -electron behavior indicating strong f - d correlation or mixing effects in the IV ground state.

II. EXPERIMENTAL PROCEDURE

Experiments in the pressure range up to 400 kbar were performed by using a gasketed diamond-cell technique.²⁵ Pressures were determined from the red shift of the ruby luminescence.²⁶ Optical reflection spectra were measured in the spectral range from 0.5 to 3.5 eV by using microoptical techniques.²⁷ In the case of YbS, samples of about 20 μm initial thickness were cleaved from single crystalline material. A small crystal was mounted with the freshly cleaved surface in direct contact with one of the diamond windows. The remaining cell volume was filled with KCl, which served as a pressure transmitting medium. Polycrystalline YbO was used without pressure medium. The high-pressure synthesis of YbO is described elsewhere.²⁸

Absolute reflectivities (denoted R_d) were measured at the diamond-sample interface. The reflectivity at the internal diamond-air interface (measured with the unloaded cell through the diamond window) provides the reference for normalizing the reflected intensities. The relative error $\Delta R_d/R_d$ arising from experimental sources (e.g., misalignment, stress-induced curvature of the diamond-sample interface) is estimated to be less than 5% at the high-pressure limit. The effect of nonisotropic stresses on the gross features of the optical spectra is believed to be negligible, because the pressure range by far exceeds the yield strength of the samples.

Powder x-ray diffraction patterns of YbS were recorded in the angle-dispersive mode using Mo $K\alpha$ radiation and a diffractometer equipped with scintillation counters. In the x-ray measurements either a 4:1 methanol-ethanol mixture or silicone fluid was used as a pressure medium.

III. EXPERIMENTAL RESULTS

Reflection spectra for YbS in the 100 kbar pressure range are shown in Fig. 1. Near normal pressure one observes two weak reflection bands separated by roughly 1.3 eV. The low-energy band exhibits a weak structure. The position of this reflectivity peak is located about 0.2 eV above the absorption edge near 1.27 eV.²⁴ The 0.2-eV energy difference does not change significantly under pressure, as evidenced by the observation of interference noise below the first reflection band. Spectra at 6 and 47 kbar in Fig. 1 are cut off at the onset of interferences.

In accordance with thin-film absorption studies of semiconducting YbX,^{23,24,29} the first transition is readily interpreted as an excitation to the $^2F_{7/2}$ spin-orbit component of $4f^{13}5d$. The splitting between the two reflection bands is close to the spin-orbit splitting of $4f^{13}$ in the free Yb ion [1.24 eV (Ref. 22)]. With increasing pressure, both bands shift almost in parallel to lower energy, which identifies the second excited state as the $^2F_{5/2}$ component of $4f^{13}5d$. From the general features of the band structures of RX (Ref. 30) and the optical properties of alkaline-earth chalcogenides³¹ at normal pressure, the threshold for direct (possibly excitonic) valence to conduction band transitions ($X'_5-X'_3$) at normal conditions is expected to be larger than 3 eV, i.e., it lies just outside the present spectral range. The indirect p - d gap ($\Gamma_{15}-X'_3$) should be closer to 2.5 eV.

The $4f$ -to- $5d$ excitation energies decrease at a rate of about -12 meV/kbar, which indicates the onset of the $4f$ - $5d$ energetic overlap near 100 kbar. As shown in Fig. 2, the reflectivity starts to increase considerably above 120 kbar and tends to saturate near 300 kbar. However, below 1 eV photon energy one finds a steep reflectivity edge, which becomes more pronounced and shifts to higher energy with increasing pressure.

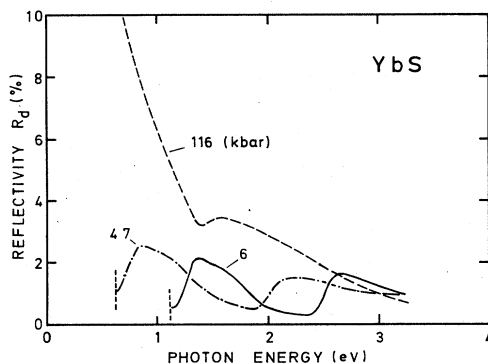


FIG. 1. Optical reflection spectra of YbS at 6, 47, and 116 kbar. The vertical dashed lines indicate the energy below which interference noise is observed.

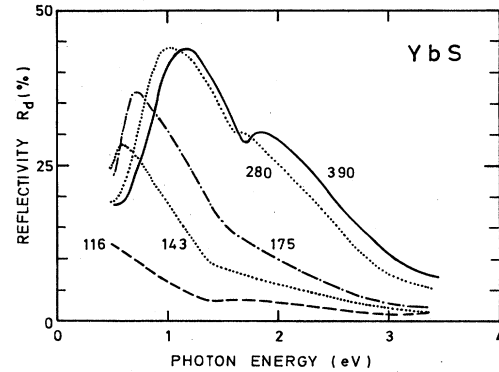


FIG. 2. Optical reflection spectra of YbS above 100 kbar. Numbers correspond to pressure in kbar. Note the change in reflectivity scale compared with Fig. 1.

Qualitatively, the changes in reflectivity of YbS and YbO under pressure are very similar. At low pressures the two weak reflection bands of YbO are not as sharp compared with YbS, which seems to be related to differences in sample quality. Reflection spectra of both compounds near 400 kbar are compared in Fig. 3. In YbO, one again finds the pronounced NIR reflectivity edge.

The data for YbS have been analyzed by using Drude-Lorentz-type oscillator expressions³² for the complex dielectric function $\epsilon(\omega) = \epsilon_1(\omega) + i\epsilon_2(\omega)$:

$$\epsilon(\omega) = \epsilon_\infty + \omega_p^2 \sum_j \frac{f_j}{\omega_j^2 - \omega^2 - i\Gamma_j \omega} \quad (1)$$

and by fitting the corresponding reflectivity

$$R_d(\omega) = \left| \frac{n_d - \epsilon^{1/2}}{n_d + \epsilon^{1/2}} \right|^2 \quad (2)$$

to the experimental spectra. With the density N of Yb ions, which is known or extrapolated from the pressure-volume (PV) relation (see below), we have $\omega_p^2 = 4\pi N e^2 / m$, where m is the free-electron mass. The parameters f_j and Γ_j represent oscillator strength and width (or phenomenological scattering rate), respectively, of the transition at

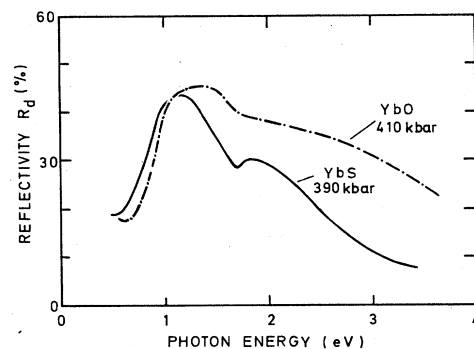


FIG. 3. Optical reflection spectra of YbO and YbS near 400 kbar.

photon energy $\hbar\omega_j$. The background dielectric constant ϵ_∞ takes into account effects of higher-energy transitions. Its value is closely related to the gap for direct valence-to-conduction-band excitations. The refractive index of diamond $n_d=2.41$ is assumed to be independent of pressure.

For spectra measured below 80 kbar we use $\epsilon_\infty=4.5$, which is the corresponding value of closely related alkaline earth sulphides.³³ With this assumption, the oscillator strengths for the transitions to ${}^2F_{7/2}$ and ${}^2F_{5/2}$ observed in YbS at low pressures is ~ 0.07 and ~ 0.04 , respectively.

Results for YbS at 390 kbar are presented in more detail in Figs. 4 and 5. Two different extrapolations were used for the infrared part of the spectrum (see Fig. 4): The reflectivity is assumed to either increase again toward high values (due to metallic behavior or other low-energy excitations) or to remain nearly constant. In accordance with results for "gold" SmS,⁹ the background dielectric constant is assumed to be lower ($\epsilon_\infty=3.5$) compared with YbS near normal conditions (see also Sec. IV). Although the absolute values of the optical conductivity (real part $\sigma_1=\omega\epsilon_2/4\pi$) and of ϵ_1 above 0.5 eV depend to some extent on the low-energy extrapolation (the major differences are indicated by dotted lines in Fig. 5) and on the choice of ϵ_∞ , the spectral characteristics are not affected. The integration of σ_1 yields an effective electron number³² $n_{\text{eff}}=0.6\pm 0.10$ per Yb ion contributing to the optical response below 3 eV. The error limit includes a variation of ϵ_∞ by ± 0.5 . Strength and width of the NIR band are $f=0.27$ and $\hbar\Gamma=0.35$ eV. The clearly resolved weak structure at about twice the energy of the NIR band has a strength $f=0.015$ and a width $\hbar\Gamma=0.3$ eV.

Figure 4 also shows the reflection spectrum $R_0(\omega)$ for a hypothetical sample-vacuum interface, which is calculated with the dielectric function obtained from the analysis of $R_d(\omega)$. The absolute values of R_d and R_0 differ consider-

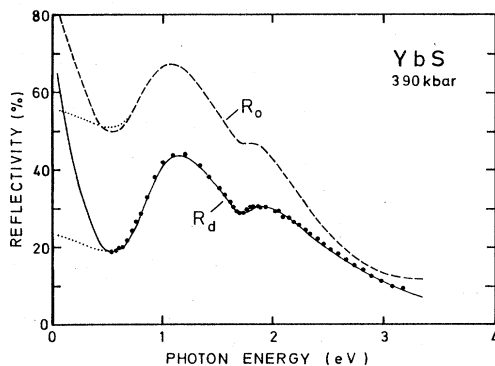


FIG. 4. Reflection spectrum of YbS at 390 kbar. Solid dots represent a selection of experimental data points. The solid line corresponds to the result of a least-squares-fit analysis (see text). The dashed curve marked R_0 represents the reflection spectrum calculated for the sample-vacuum interface. Dotted lines represent a different extrapolation of the experimental data.

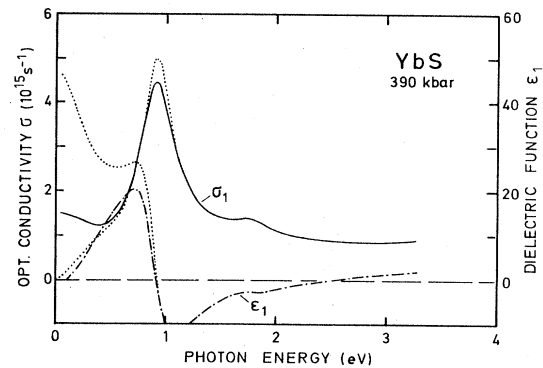


FIG. 5. Optical response functions for YbS at 390 kbar. Solid and dash-dotted lines represent the real part of the optical conductivity and dielectric function, respectively. Dotted lines correspond to results obtained for a different extrapolation of the infrared reflectivity (see dotted line in Fig. 4).

ably, because the phase shift of the reflected amplitude is affected by the large refractive index of diamond.

The analysis of the reflection spectrum at 390 kbar, as well as other spectra of YbS taken above 150 kbar, shows that the basic features of the optical response consist of a broad absorption background and a pronounced NIR absorption band. This band increases in strength and exhibits a blue shift with increasing pressure. It is obvious from a comparison of reflection spectra in Fig. 3 that YbO shows a very similar behavior. The higher reflectivity of YbO toward the high-energy end is attributed to a lower value of ϵ_∞ as compared with YbS.

Optical excitation energies in YbS are plotted in Fig. 6 as a function of pressure. The energies correspond to relative maxima of ϵ_2 given by the position of the corresponding oscillator. In cases where structure in the reflection spectra occurs very close to the low-energy experimental limit, the transition energy is estimated from the position of the reflectivity edge. The average pressure coefficients corresponding to the solid lines drawn through the low-pressure data in Fig. 6 are given in Table I.

According to previous x-ray diffraction experiments,

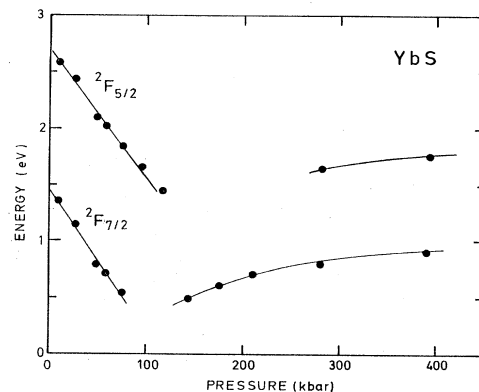


FIG. 6. Optical transition energies in YbS as a function of pressure. Energies correspond to maxima in the imaginary part of the dielectric function.

YbS shows anomalous compression behavior above 150 kbar.¹⁹ Since the optical data indicate a major change in electronic structure closer to 100 kbar, we have redetermined the pressure-volume (PV) relation. Experimental data are shown in Fig. 7. The scatter of data points reflects the combined error from lattice parameter and pressure measurement. Within a single phase region the PV relation of "normal" solids may be represented by a semi-empirical first order Birch relation,³⁴ which describes the PV behavior in terms of two parameters B_0 and B'_0 corresponding to bulk modulus and its pressure derivative, respectively, at normal conditions. Assuming $B'_0=4$ the PV data of YbS below 80 kbar yield $B_0=600\pm 30$ kbar. Provided there is no significant configuration mixing in YbS below 80 kbar, the corresponding dashed line marked "divalent" in Fig. 7 serves as an approximate reference for YbS, if it would remain truly divalent at higher pressures. Parameters for the hypothetical PV relation of "trivalent" YbS are estimated from systematic trends among trivalent RX.^{35,36} We use $V_0=24.0$ cm³/mol, $B_0=1.02$ Mbar, and $B'_0=4$, where V_0 and B_0 are chosen according to results for ErS.³⁶

Based on the above PV relation, Fig. 8 shows optical transition energies in YbS as a function of volume change. The volume coefficients corresponding to the slope of solid lines drawn through data below 100 kbar are given in Table I.

IV. DISCUSSION

We start out with the results obtained for YbS below 100 kbar. The two excitations to $^2F_{7/2}$ and $^2F_{5/2}$ may be considered as atomic-like transitions or $f-d$ excitons. The excitonic character is supported by resonant Raman scattering studies in YbS.³⁷ The corresponding excitations in other divalent RX are also enhanced by excitonic effects.³⁸ The weak structure observed in the first reflection peak is possibly related to further splitting of $4f^{13}5d$ due to $f-d$. Coulomb interactions and $5d$ electron spin-orbit coupling,³⁹ but other explanations may be possible. At normal pressure the 50% threshold for photoconductivity in YbS coincides with the optical absorption edge,²⁴ which in turn is ~ 0.2 eV below the first excitonic peak. Thus, YbS behaves different from the SmX, where the absorption edge is roughly 0.5 eV below the first $f-d$ exciton peak.⁹

The average pressure coefficient of the first optical excitation in YbS is considerably larger compared with a previous result²³ (see Table I) obtained from absorption measurements in the 10-kbar pressure range. Unless we

TABLE I. Average pressure and volume coefficients for optical $4f^{14}\rightarrow 4f^{13}(2F_j)5d$ excitations in YbS at pressures below 80 kbar.

Transition	E_0 (eV)	$(dE/dP)_{av}$ (meV/kbar)	$dE/d \ln V$ (eV)
$^2F_{7/2}$	1.49 ± 0.04	-12.5 ± 1.5 6.0 ± 1.5^a	10.0 ± 1.5 4.3^a
$^2F_{5/2}$	2.73 ± 0.04	-11.5 ± 1.5	9.2 ± 1.5

^aReferences 1 and 23.

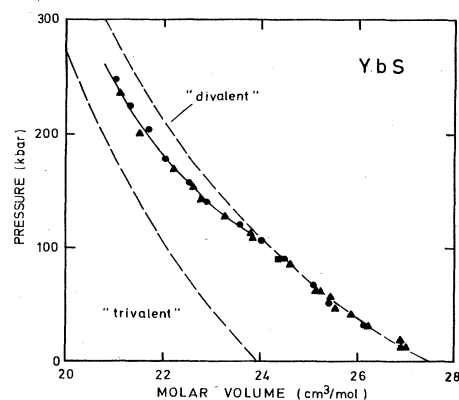


FIG. 7. Pressure-volume relation of YbS. Closed circles and triangles represent runs with silicone oil and methanol-ethanol pressure medium, respectively. Solid line is a guide to the eye. For dashed lines see text.

have overlooked some more subtle effects in the low pressure range, a possible explanation of this large difference may be, that the thin films used in the absorption study were supported by a substrate. The bulk modulus $B_0=600$ kbar from the present study is somewhat smaller compared with the result of Ref. 19 ($B_0=720+50$ kbar), but consistent with an Anderson-Nafe plot for the closely related alkaline earth chalcogenides.⁴⁰

The PV relation of YbS clearly exhibits an anomalous behavior starting just around 100 kbar, which supports the onset of a noticeable $f-d$ mixing near this pressure. From a lattice parameter scaling (Vegard's law) the mean valence is roughly 2.4 at 250 kbar. However, the uncertainty is as large as ± 0.15 , because at high pressures the divalent and trivalent reference volumes are not well established. The slope of the experimental PV data above 150 kbar suggests that the approach to the trivalent reference curve tends to saturate, so that the mean valence near 400 kbar is estimated to be roughly 2.5. The mean valence of YbO near 350 kbar as estimated from the PV

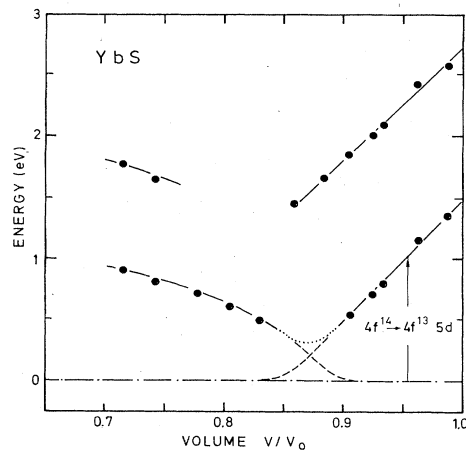


FIG. 8. Optical transition energies in YbS as a function of relative volume.

data of Ref. 20 is less than 2.6. Thus, there seems to be no significant difference in the $4f$ occupation in YbO and YbS at about 400 kbar, which is the highest pressure of the optical measurements. This view is supported by the close similarity in optical reflectivity (see Fig. 3).

We now turn to the discussion of the optical response of YbS and YbO above 150 kbar. It is convenient to first summarize some features of the optical properties of related SmX and TmX. A general experimental observation for IV SmX and TmX is the overall enhancement of optical transitions at photon energies below roughly 2 eV as compared with the semiconducting divalent state. The enhancement is expected to occur at least partly at the expense of valence to conduction-band excitations, because the occupied $5d$ states are no longer available as final states for p - d transitions and any excitonic effects near the p - d threshold are likely to be screened. Evidence for this may be found from a comparison of the dielectric functions for semiconducting and "gold" SmS as given in Ref. 9. Thus, the background dielectric constant for the visible and infrared spectral range is expected to decrease in going from the divalent to the IV state.

A further common feature of the low-energy optical response of all IV SmX and TmX is a smooth metallic-like reflectivity in the NIR spectral range followed by a plasma reflection edge in the visible.⁹⁻¹⁵ In SmS and TmSe, which both show IV behavior at normal conditions or low pressure, more complicated optical properties are observed only at photon energies below ~ 0.2 eV.^{9,11-13} The reflection spectrum of nearly trivalent SmS at 250 kbar shown in Fig. 9 demonstrates that no strongly anomalous features are induced at very high pressures.⁴¹ During the continuous valence change in SmSe and SmTe, a plasma reflection edge shifts from the NIR to the visible with increasing pressure.^{14,15} The spectra in Fig. 9 demonstrate this effect for TmTe.⁴¹ Obviously, the energetic position of the plasma edge and therefore the total

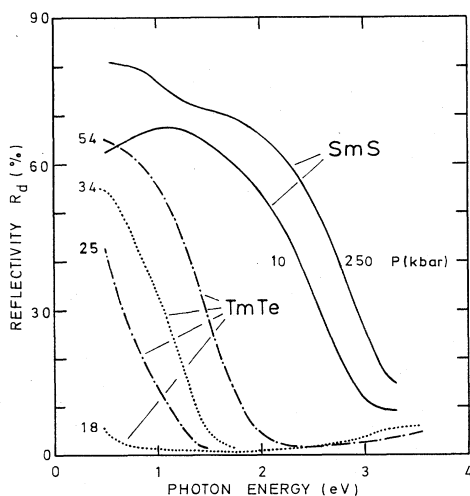


FIG. 9. Optical reflection spectra of SmS and TmTe at different pressures. All spectra have been measured at the sample-diamond interface.

oscillator strength for optical transitions at photon energies below roughly 3 eV is closely related to the amount of d admixture in the IV ground state of SmX and TmX. As a systematic trend the energetic position of the reflection edge for a given $5d$ occupation shifts to lower energy in going from sulphide to telluride, i.e., with increasing screening due to p - d transitions.

Most of the explanations for the optical response of SmX and TmX are based on a "band-type" description of the IV state. The electronic structure is characterized by a sharp $4f$ - $5d$ resonance at the Fermi level E_F and the position of E_F above the bottom of the $5d$ band at the X point is determined by filling the structureless free-electron-like $5d$ density of states according to the fractional occupancy of $4f^n 5d$ [Fig. 10(a)]. The high reflectivity is then attributed to a Drude-type intraband term for electrons transferred to delocalized $5d$ states.^{9,11,13} According to Ref. 12, the far-infrared properties and the small optical gap (7 meV wide) of "gold" SmS are consistent with a band-type model, because a continuous distribution of d - f interband excitations spanning the energy range from roughly 0.2 to 2 eV explains the metallic appearance equally well.

Similar to the optical response of IV SmX and TmX, both YbS and YbO exhibit an overall increase of the reflectivity and thus an enhancement of low-energy optical transitions starting near 120 kbar. It is the NIR reflectivity edge and the corresponding absorption band, which makes the high-pressure optical response of YbS and YbO strikingly different from all IV SmX and TmX. The NIR band in YbO and YbS appears to be characteristic of the Yb ion. A crystal structure effect can be excluded, because the NaCl-type phase of YbS and YbO is stable up to at least 250 kbar (see above) and 350 kbar,¹¹ respectively.

A possible explanation of the NIR band is suggested by the dependence of optical transitions on volume as shown in Fig. 8. There, the dashed lines illustrate how the initial and final states of the NIR transition in the IV phase are thought to emerge from the f -to- d excitation at low pressures. The interpretation is that the excitonic (or localized) $4f^{13}5d$ final state of the optical excitation spectrum below 100 kbar develops into a narrow $4f^{13}5d$ component in the IV ground state above 100 kbar. Similarly, the final state of the NIR band acquires more $4f^{14}$ character with increasing pressure. The oscillator strength of the

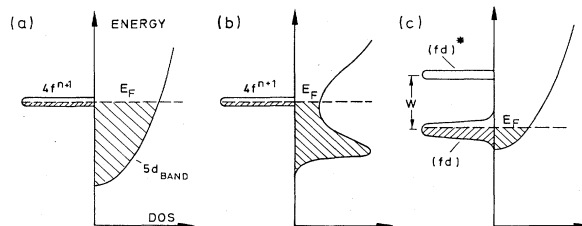


FIG. 10. Schematic energy level diagrams representing different descriptions of the intermediate-valence situation in rare-earth monochalcogenides. See text for details.

NIR transition increases with pressure, which suggests an increasing occupation of the narrow $5d$ component. Near 400 kbar this oscillator strength ($f=0.27$) is about 2.5 times larger compared to the combined strengths ($f=0.11$) of the f - d transitions at $P < 60$ kbar.

In a band-type description the formation of a narrow d component in the IV ground state may be attributed to the Coulomb interaction between $4f$ hole and $5d$ electron, thus reducing the free-electron-like nature of the d electrons. As pointed out by Lawrence *et al.* (see Chap. 3.9 of Ref. 4) a localized $5d$ component may be expected near the conduction-band edge [schematically indicated in Fig. 10(b)]. In this case, we would attribute the NIR band to excitations from predominantly $5d$ -like states near the bottom of the conduction band to narrow final $4f$ states near E_F . The relatively weak dependence of this d -to- f transition energy on volume at pressures above 200 kbar would then reflect a tendency toward saturation of the valence change, as is also evidenced by the PV relation. Within the band-type approach, a strong fd mixing or hybridization effect would be an alternative or additional mechanism leading to the formation of a narrow d component and, furthermore, to a minimum in the sd -like density of states near E_F , as also indicated in Fig. 10(b).

On the other hand, inspired by the "excitonic" ground-state model of Kaplan and co-workers⁴² (see also Schweitzer⁴³), one may also consider a situation with predominantly localized energy levels in the IV state. A schematic picture is given in Fig. 10(c). The narrow occupied and empty states, denoted (fd) and $(fd)^*$, both have $4f^{n+1}$ and $4f^n 5d$ character, and the relative weight of the two contributions in the ground state determines the mean valence. The two narrow states are separated by a gap with the gap energy W depending in part on the strength of the mixing interaction. Kaplan *et al.*⁴² assume that the $4f^n 5d$ admixture is strongly localized and that configuration mixing between $4f^{n+1}$ and $4f^n 5d_{loc}$ arises from an interatomic dipole interaction. Furthermore, in their model a broad $5d$ conduction band, which is occupied by no more than 0.1 electrons per RE ion, overlaps both localized components [see Fig. 10(c)]. In this picture, the NIR absorption band in YbS could be attributed to transitions between the narrow (fd) and $(fd)^*$ states.

The strongly localized description of the IV ground state in YbS would imply a relatively large fd mixing interaction and a large spread in the $4f^{14}$ weight, the latter increasing to roughly 1 eV at 400 kbar.

Although the present results strongly support a localized d -electron behavior, they do not allow for an unambiguous distinction between a band-type situation with strong fd correlation or mixing effects [Fig. 10(b)] and a predominantly localized picture with an extremely wide spread of $4f^{14}$ weight [Fig. 10(c)]. If we assume that the oscillator strength of the NIR band is an approximate measure of the localized d admixture in the ground state,

the population of narrow $5d$ states in IV YbS and YbO would be appreciable, regardless of the particular model involved in the interpretation.

We emphasize that the schematic representations in Figs. 10(b) and 10(c) are meant to illustrate possible interpretations of the optical response of YbS (and YbO) in the IV state at photon energies above 0.5 eV. Optical properties on a smaller energy scale and, in particular, the question of metallic or insulating IV ground state in YbS remain to be investigated. In this context it should be noted that the volume dependence of the optical transitions in YbS points to the possible existence of an approximately 0.3-eV wide direct optical gap near 100 kbar, as indicated by the dotted line in Fig. 8. Optical experiments extending below 0.5-eV photon energy are needed to further elucidate the pressure dependence of energy levels at pressures near the onset of fd mixing.

The second weak absorption band in the reflection spectra taken at the highest pressures possibly emerges from the transition to the $^2F_{5/2}$ excited state observed at low pressures. It can, however, not be related to the first NIR transition on the basis of the $4f^{13}$ spin-orbit splitting in the free Yb ion.

As pointed out in the Introduction, the Yb ion differs from Sm and Tm ions by its simple $4f$ multiplet structure and by a larger third ionization potential. The multiplet structure of the Yb ion is certainly favorable for an optical detection of localized d -electron behavior. The larger third ionization potential of the Yb ion possibly implies a larger excitonic f - d interaction in the divalent as well as in IV state. Another consequence of the larger ionization potential is that the separation between p valence bands and $4f$ states is smaller, which may result in stronger covalent effects. It remains to be considered in more detail, whether p - f mixing can have an effect on the optical properties of IV YbX at photon energies below 2 eV.

V. CONCLUSIONS

We summarize the present results as follows:

- (i) Below 80 kbar, the lowest $4f^{14}$ to $4f^{13}5d$ excitations in YbS decrease with pressure at an average rate of roughly -12 meV/kbar. Optical reflection spectra indicate the onset of a $4f$ - $5d$ energetic overlap near 100 kbar.
- (ii) Lattice parameter measurements of YbS under pressure reveal a compression anomaly starting near 100 kbar, which is consistent with a continuous onset of $4f$ - $5d$ mixing at this pressure.
- (iii) The optical response of YbS in the IV phase is different from that of related Sm and Tm compounds by showing a pronounced pressure-dependent absorption band between 0.5- and 1-eV photon energy, which is also observed in YbO.
- (iv) This absorption band is interpreted as a signature of a localized d component in the IV ground state.

¹A. Jayaraman, in *Handbook on the Physics and Chemistry of the Rare Earth*, edited by K. A. Gschneidner and L. Eyring (North-Holland, Amsterdam, 1979), Vol. 2, p. 575.

²B. Johansson, *Phys. Rev. B* **12**, 3253 (1975).

³C. M. Varma, *Rev. Mod. Phys.* **48**, 219 (1976).

⁴J. M. Lawrence, P. S. Riseborough, and R. D. Parks, *Rep. Prog. Phys.* **44**, 1 (1981). See also for references to other reviews.

- ⁵*Valence Instabilities and Related Narrow Band Phenomena*, edited by R. D. Parks (Plenum, New York, 1976).
- ⁶*Valence Fluctuations in Solids*, edited by L. M. Falicov, W. Hanke, and M. B. Maple (North-Holland, New York, 1981).
- ⁷*Valence Instabilities*, edited by P. Wachter and H. Boppert (North-Holland, Amsterdam, 1982).
- ⁶*Valence Fluctuations in Solids*, edited by L. M. Falicov, W. Hanke, and M. B. Maple (North-Holland, New York, 1981).
- ⁷*Valence Instabilities*, edited by P. Wachter and H. Boppert (North-Holland, Amsterdam, 1982).
- ⁸*Proceedings of the International Conference on Valence Fluctuations, Köln, 1984*, edited by B. Roden, E. Müller-Hartmann, and D. Wohlleben [J. Magn. Magn. Mater. **47& 48** (1985)].
- ⁹B. Batlogg, E. Kaldis, A. Schlegel, and B. Wachter, Phys. Rev. B **14**, 653 (1976); contains references to earlier optical studies of SmS.
- ¹⁰G. Güntherodt, R. Keller, P. Grünberg, A. Frey, W. Kress, R. Merlin, W. B. Holzapfel, and F. Holtzberg, in *Valence Instabilities and Related Narrow-Band Phenomena*, Ref. 5, p. 321.
- ¹¹J. W. Allen, R. M. Martin, B. Batlogg, and P. Wachter, J. Appl. Phys. **49**, 2078 (1978).
- ¹²P. Wachter and G. Travaglini, in Proceedings of the International Conference on Valence Fluctuations, Köln, 1984, Ref. 8.
- ¹³B. Batlogg, Phys. Rev. B **23**, 1827 (1981).
- ¹⁴B. Welber and A. Jayaraman, J. Appl. Phys. **50**, 462 (1979).
- ¹⁵K. Syassen, J. Phys. (Paris) Colloq. **45**, C8-123 (1984).
- ¹⁶L. R. Morss, J. Phys. Chem. **75**, 393 (1971).
- ¹⁷A. Jayaraman, Phys. Rev. Lett. **29**, 1674 (1972).
- ¹⁸A. Chatterjee, A. K. Singh, and A. Jayaraman, Phys. Rev. B **6**, 2285 (1972).
- ¹⁹A. Jayaraman, A. K. Singh, A. Chatterjee, and S. U. Devi, Phys. Rev. B **9** 2513 (1974).
- ²⁰A. Werner, H. D. Hochheimer, A. Jayaraman, and J. M. Leger, Solid State Commun. **38**, 325 (1981).
- ²¹H. G. Zimmer, K. Takemura, K. Syassen, and K. Fischer, Phys. Rev. B **29**, 2350 (1984).
- ²²G. H. Dieke, *Spectra End Energy Levels of Rare Earth Ions in Crystals* (Wiley, New York, 1968).
- ²³V. Narayanamurti, A. Jayaraman, and E. Bucher, Phys. Rev. B **9**, 2521 (1974).
- ²⁴L. N. Glurdzhidze, T. D. Kekhainov, D. G. Gzirishvili, T. L. Bzhalava, and V. V. Sanadze, Fiz. Tverd. Tela (Leningrad) **22**, 660 (1980) [Sov. Phys. Solid State **22**, 388 (1980)].
- ²⁵For a review see A. Jayaraman, Rev. Mod. Phys. **55**, 65 (1983).
- ²⁶G. J. Piermarini, S. Block, J. D. Barnett, and R. A. Forman, J. Appl. Phys. **46**, 2774 (1975).
- ²⁷K. Syassen and R. Sonnenschein, Rev. Sci. Instrum. **53**, 644 (1982).
- ²⁸J. M. Leger, J. Maugrion, L. Albert, J. C. Achard, and C. Loriers, C. R. Acad. Sci. Paris **201**, 2860 (1978).
- ²⁹R. Suryanarayanan, J. Ferre, and B. Briat, Phys. Rev. B **9**, 554 (1974).
- ³⁰*Landolt-Börnstein Numerical Data and Functional Relationships in Science and Technology*, New Series, edited by K. H. Hellwege (Springer, Berlin, 1982), Vol. III/17g.
- ³¹R. J. Zollweg, Phys. Rev. **111**, 113 (1958); G. A. Saum and E. B. Hensley, *ibid.* **113**, 1019 (1959); Y. Kaneko, K. Morimoto, and T. Koda, J. Phys. Soc. Jpn. **52**, 4385 (1983).
- ³²See, e.g., F. Wooten, *Optical Properties of Solids* (Academic, New York, 1972).
- ³³*CRC Handbook of Chemistry and Physics*, edited by R. C. Weast, 65th ed. (CRC Press, Boca Raton, 1984).
- ³⁴F. Birch, J. Geophys. Res. **83**, 1257 (1978).
- ³⁵J. M. Leger, N. Yacoubi, and C. Loriers, J. Solid State Chem. **36**, 261 (1981).
- ³⁶A. Jayaraman, B. Batlogg, R. G. Maines, and H. Bach, Phys. Rev. B **26**, 3347 (1982).
- ³⁷R. Merlin, G. Güntherodt, R. Humphreys, M. Cardona, R. Suryanarayanan, and F. Holtzberg, Phys. Rev. B **17**, 4951 (1978).
- ³⁸C. Mariani, S. Modesti, R. Rosei, F. Simoni, and E. Tosatti, Solid State Commun. **38**, 833 (1981).
- ³⁹F. Anisimov, R. Dagys, and A. Sargautis, Int. J. Quantum Chem. **24**, 429 (1983); see also Liet. Fiz. Rinkiny **19**(3), 377 (1979) [Sov. Phys.—Coll. **19**, 22 (1979)].
- ⁴⁰H. G. Zimmer, H. Winzen, and K. Syassen, Phys. Rev. B (to be published).
- ⁴¹A more detailed discussion of pressure-induced changes in the optical response of TmTe and SmX is in preparation. The pressure range for the TmTe optical spectra in Fig. 9 is limited to 54 kbar, because a structural transition starts to interfere at higher pressures.
- ⁴²T. A. Kaplan, S. D. Mahanti, and M. Barma, in *High Pressure and Low Temperature Physics*, edited by C. W. Chu and J. A. Woolham (Plenum, New York, 1978), p. 141; *Valence Instabilities and Related Narrow Band Phenomena*, Ref. 5, p. 153.
- ⁴³J. W. Schweitzer, Phys. Rev. B **13**, 3506 (1976).